Ultrafast nonequilibrium carrier dynamics in a single graphene layer

M. Breusing,[1] S. Kuehn,[1] T. Winzer,[2] E. Malić,[2] F. Milde,[2] N. Severin,[3] J. P. Rabe,[3]
C. Ropers,[4] A. Knorr,[2] and T. Elsaesser[1,*]

[1]*Max-Born-Institut für Nichtlineare Optik und Kurzzeitspektroskopie, D-12489 Berlin, Germany*
[2]*Institut für Theoretische Physik, Nichtlineare Optik und Quantenelektronik, Technische Universität Berlin, D-10623 Berlin, Germany*
[3]*Institut für Physik, Humboldt Universität zu Berlin, D-12489 Berlin, Germany*
[4]*Courant Research Center, Universität Göttingen, D-37077 Göttingen, Germany*

(Received 19 January 2011; published 19 April 2011)

Nonequilibrium carrier dynamics in single exfoliated graphene layers on muscovite substrates are studied by ultrafast optical pump-probe spectroscopy and compared with microscopic theory. The very high 10-fs-time resolution allows for mapping the ultrafast carrier equilibration into a quasi-Fermi distribution and the subsequent slower relaxation stages. Coulomb-mediated carrier-carrier and carrier-optical phonon scattering are essential for forming hot separate Fermi distributions of electrons and holes which cool by intraband optical phonon emission. Carrier cooling and recombination are influenced by hot phonon effects.

DOI: 10.1103/PhysRevB.83.153410 PACS number(s): 78.40.Kc, 63.22.Rc, 78.47.J−, 81.05.ue

Graphene consisting of a single layer of carbon atoms arranged in a honeycomb lattice represents a two-dimensional model system that has received tremendous attention, both from the viewpoint of basic physics and for device applications.[1–4] The electronic band structure of graphene displays a vanishing energy gap at the three K and the three K' points in $\mathbf{k}$ space, characteristic for a zero-band-gap semiconductor.[5] The nonequilibrium dynamics of carriers in graphene are essential for understanding electronic transport and optical properties. Electronic transport in graphene has been studied in substantial detail with, e.g., both electrons and holes contributing to the remarkably high carrier mobility at room temperature ($T = 300\,\mathrm{K}$).[6–8]

Nonequilibrium carrier dynamics are governed by microscopic interactions, such as Coulomb-mediated carrier-carrier scattering and scattering of carriers with optical and acoustic phonons, both occurring within and between the valence and conduction bands. So far, there is limited insight into the femtosecond time scales and interplay of such processes in carrier relaxation in graphene. As a result, it is unclear how highly energetic nonequilibrium electrons and holes relax into quasiequilibrium carrier distributions and if such equilibration follows a relaxation scenario characteristic for a metal or for a semiconductor. The nature of the relaxation processes can be mapped in real time by optical methods with a femtosecond time resolution, allowing for a separation of the different microscopic steps and a direct comparison of experimental findings with theoretical simulations.

Ultrafast optical experiments have elucidated different aspects of carrier and lattice dynamics in graphite, representing a stack of many graphene layers.[9–15] Recent work on single and few layer graphene on different substrates revealed relaxation dynamics of photoexcited electrons dependent on the number of layers with the shortest time constant of about 150 fs for single layer graphene.[16–19] However, the temporal resolution was insufficient to resolve the formation dynamics of a quasiequilibrium distribution and to separate this process from slower carrier cooling and recombination processes.

In contrast to earlier work, we investigate a single graphene layer and present a unique combination of a high-resolution pump-probe experiment with microscopic calculations offering insights into time- and momentum-resolved carrier relaxation dynamics. Graphene was prepared on an atomically flat, optically transparent muscovite (mica) substrate, resulting in a high structural quality. Ultrafast pump-probe experiments with an unprecedented time resolution of 10 fs map the early stages of carrier relaxation and identify the characteristic time scale of carrier equilibration by Coulomb and optical phonon scattering. The influence of the different many-particle contributions is clearly distinguished in the microscopic calculations of the time evolution.

In our experiments, we studied exfoliated graphene layers supported by freshly cleaved mica as shown in Fig. 1(a). Samples were prepared at low humidity (<10 ppm H_2O) in a glove box to minimize a potential water contamination of the graphene-mica interface.[20] The presence of just one layer of graphene was verified by reflectivity measurements[21] and confocal Raman spectroscopy, the latter giving evidence for a single peak structure of the Raman 2D band.[22,23] For the dynamic measurements, the sample is kept in a chamber rinsed with nitrogen, lowering the amount of oxygen to below 1%.

Femtosecond pump-probe experiments were performed in a transmission geometry [Fig. 1(a)], where the linearly polarized pump pulse centered at 1.5 eV (bandwidth 0.6 eV; cf. with the pulse spectrum in the upper panel of Fig. 2) excites electron-hole pairs via interband transitions [Fig. 1(b)]. The resulting transmission change is mapped with a probe pulse centered at the same spectral position and polarized perpendicularly to the pump. The transmitted probe light was isolated with a polarizer and detected either spectrally integrated or spectrally resolved with a monochromator and a photodiode. Noncollinear pump and probe pulses of 7 fs duration were derived from a mode-locked Ti:sapphire oscillator working at a 71 MHz repetition rate and focused onto the sample through a reflective microscope objective. The spot size was approximately $5 \times 5\ \mu\mathrm{m}^2$. A pump fluence of $0.2\ \mathrm{mJ/cm^2}$ corresponds to a carrier density of approximately

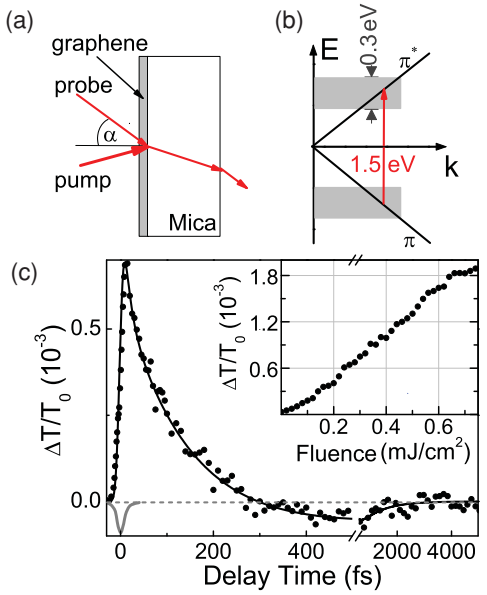

FIG. 1. (Color online) (a) Structure of the graphene layer on mica. The incident probe light hits the surface at an angle $\alpha = 35^\circ$. (b) Schematic linear band structure of graphene, the arrow indicating the pumped and probed optical transitions. (c) Spectrally integrated transmission change (points) as a function of pump-probe delay. Solid line: biexponential fit. Gray line: cross correlation of pump and probe pulses. Inset: linear dependence of the maximum transmission change on pump fluence.

2×10^{13} cm^{-2} generated in single layer graphene with a linear absorption coefficient $a_0 = \frac{e^2}{4\epsilon_0 \hbar c} \approx 2.3\%$.[24]

Results of the time-resolved experiments are presented in Figs. 1 and 2. In Fig. 1(c), the spectrally integrated transmission change $\Delta T/T_0 = (T - T_0)/T_0$ is plotted as a function of pump-probe delay (T, T_0: sample transmission with and without excitation). The sample displays an ultrafast transmission increase within the time resolution of the experiment and a fast decay on a time scale of several hundreds of femtoseconds.

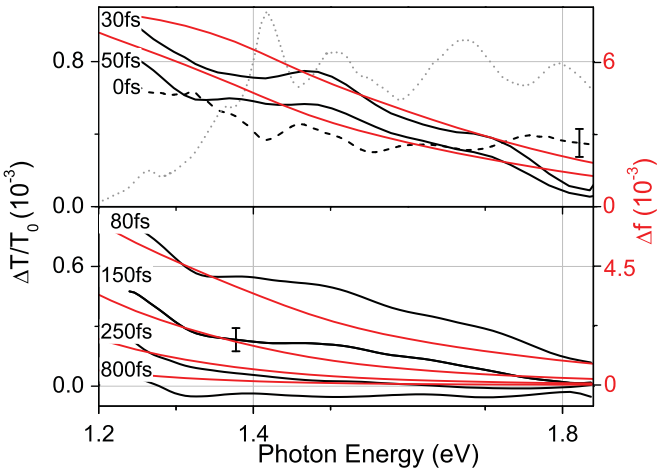

FIG. 2. (Color online) Spectrally resolved transmission change as a function of probe photon energy for different delay times [black (thick) lines]. Dotted line: spectrum of the pump pulses. Red (thin) lines: corresponding simulated carrier distribution changes Δf.

Around 300 fs, the transmission change becomes negative and subsequently relaxes to 0 within a few picoseconds. A linear relation between the maximum positive transmission change and the pump fluence exists up to fluence values of 0.6 mJ/cm^2 [inset of Fig. 1(c)]. The solid line through the data points represents a numerical fit of the time evolution, consisting of an initial decay with a time constant of 140 fs and a slower decay of the negative signal with a time constant of 0.8 (−0.3/+1.5) ps. In Fig. 2, the transmission change $\Delta T/T_0$ is plotted as a function of photon energy (within the probe spectrum) for different pump-probe delays (black lines). Starting from the spectrally more or less constant transmission change at 0 fs (dashed black line), the spectra evolve toward an essentially monotonous increase of $\Delta T/T_0$ to smaller photon energies.

Next, we discuss the results in more detail. The femtosecond pump pulse excites carriers from the valence to the conduction band via dipole-allowed $\pi - \pi^*$ transitions around the K and K' points of the band structure. The photoexcited carriers block the corresponding interband transitions and cause a decrease of absorption due to state filling which results in the transmission increase $\Delta T/T_0$ at early delay times. Electrons and holes contribute equally to $\Delta T/T_0$ due to the identical valence and conduction band structure. Carrier redistribution leads to a change of $\Delta T/T_0$ and governs its time evolution. In a single particle picture, adiabatically eliminating polarization effects, the measured $\Delta T/T_0$ is given by

$$\frac{\Delta T(\hbar\omega)}{T_0} \approx -\Delta\alpha(\hbar\omega) = -a_0 \left(\Delta f_e\left(\frac{\hbar\omega}{2}\right) + \Delta f_h\left(-\frac{\hbar\omega}{2}\right)\right), \quad (1)$$

where $\Delta f_{e,h}(\hbar\omega,t) = f_{e,h}(\hbar\omega,t) - f_{e,h}(\hbar\omega, -\infty)$ is the difference between the momentary distribution function $f_{e,h}(\hbar\omega,t)$ of electrons and holes at time t and energy $\hbar\omega$ and the distribution functions $f_{e,h}(\hbar\omega, -\infty)$ prior to excitation. Compared to $\Delta T/T_0$, changes of the reflectivity of the graphene layer are negligible.[24,25]

In our experiment, transient valence and conduction band populations are probed at energies which are approximately 0.75 eV below and above the K and K' points. The nonequilibrium carriers excited by the pump pulse undergo a fast equilibration process, spreading them over a wide energy range down to the K and K' points and establishing a hot quasiequilibrium Fermi distribution. During the initial equilibration period, the photoexcited carriers can induce Auger processes which promote electrons from valence to low-lying conduction band states and enhance the total carrier density.[26] After equilibration, the population of the optically probed states, which are well above/below the quasi-Fermi levels of electrons/holes, is governed by the transient carrier temperature which decreases by carrier cooling via optical phonon emission. Both carrier equilibration and cooling result in a decrease of the population of the optically probed states and a concomitant decrease of the measured $\Delta T/T_0$.

The spectrally integrated $\Delta T/T_0$ [Fig. 1(c)] reflects the total population of states in the optical window, decaying completely within 300 fs. The subsequent negative $\Delta T/T_0$ will be discussed below. In contrast, the spectrally resolved $\Delta T/T_0$ (Fig. 2) gives insight into the momentary carrier

distribution [cf. Eq. (1)]. The spectrum taken at a 0 fs delay displays a transmission change that—within the experimental accuracy—is independent of photon energy. This shape is a clear indication of a distinctly nonthermal carrier distribution. Within the next 50 fs, the spectra develop an increase toward small photon energies, reflecting the ultrafast redistribution of carriers, i.e., the initial phase of equilibration into hot Fermi distributions of electrons and holes. At delays longer than 200 fs, the spectra increase toward lower energies, with a decreasing amplitude as a function of delay time. Such behavior is characteristic for the cooling of a hot Fermi distribution and allows for deriving the momentary carrier temperature.

This interpretation is supported by a theoretical investigation, where a time-, angle-, and momentum-resolved simulation of carrier dynamics is performed. Using the Heisenberg equation and a second-order Born-Markov approximation, the Bloch equations for graphene read[27]

$$\dot{p}_{\mathbf{k}}(t) = -i\,\Delta\omega_{\mathbf{k}}\,p_{\mathbf{k}} - i\,\Omega(f^{e}_{\mathbf{k}} + f^{h}_{\mathbf{k}} - 1) - \mathcal{T}_{\mathbf{k}}\;p_{\mathbf{k}} + \mathcal{U}_{\mathbf{k}}, \quad (2)$$

$$\dot{f}^{\lambda}_{\mathbf{k}}(t) = 2\mathrm{Im}(\Omega p^{*}_{\mathbf{k}}) + \mathcal{S}^{\mathrm{in}}_{\mathbf{k},\lambda}(1 - f^{\lambda}_{\mathbf{k}}) - \mathcal{S}^{\mathrm{out}}_{\mathbf{k},\lambda} f^{\lambda}_{\mathbf{k}}, \quad (3)$$

$$\dot{n}^{j}_{\mathbf{q}}(t) = -\gamma(n^{j}_{\mathbf{q}} - n_0) + \mathcal{P}^{\mathrm{in}}_{\mathbf{q},j}(n^{j}_{\mathbf{q}} + 1) - \mathcal{P}^{\mathrm{out}}_{\mathbf{q},j} n^{j}_{\mathbf{q}}. \quad (4)$$

These equations (similar to semiconductor Bloch equations [28]) describe the coupled temporal evolution of the coherence $p_{\mathbf{k}}$ and carrier population $f^{\lambda}_{\mathbf{k}}$ at the momentum $\mathbf{k}$ for electrons (e) and holes (h), where $\lambda = e,h$, as well as the occupation number of optical phonons $n^{j}_{\mathbf{q}}$ with the wave vector $\mathbf{q}$ and the Γ and K phonon branch $j = \Gamma_{LO/TO}, K_{LO/TO}$.[27] The optical transition energy is given by the band structure $\hbar\Delta\omega_{\mathbf{k}} = \varepsilon^{e}_{\mathbf{k}} + \varepsilon^{h}_{\mathbf{k}}$. The carrier-light interaction couples the coherence to the carrier population via the Rabi frequency $\Omega = i\frac{e}{m}\mathbf{M}^{vc}_{\mathbf{k}}\mathbf{A}(t)$, where $\mathbf{M}^{vc}_{\mathbf{k}}$ is the wave number dependent optical matrix element for graphene.[29,30] The laser pulse is described by the vector potential $\mathbf{A}(t)$ that drives the system. The decay of the phonon population is incorporated by a phenomenological damping term $-\gamma(n^{j}_{\mathbf{q}} - n_0)$,[27] where n_0 is the Bose-Einstein distribution at room temperature and $\gamma^{-1} = 1.2$ ps corresponds to the lifetime of the phonons determined recently.[31] The contributions of the two-particle interactions result in Boltzmann-like scattering equations including Pauli blocking terms with $\mathcal{S}^{\mathrm{in/out}}_{\mathbf{k},\lambda} = \mathcal{S}^{\mathrm{in/out},C}_{\mathbf{k},\lambda} + \mathcal{S}^{\mathrm{in/out},P}_{\mathbf{k},\lambda}$. The rates for the Coulomb scattering ($\mathcal{S}^{\mathrm{in/out},C}_{\mathbf{k},\lambda}$ [32]) and the phonon induced dynamics ($\mathcal{S}^{\mathrm{in/out},P}_{\mathbf{k},\lambda}$ and $\mathcal{P}^{\mathrm{in/out}}_{\mathbf{q},j}$[27]) are computed as a function of time. The two-particle contributions to the decoherence are $\mathcal{T}_{\mathbf{k}}$, representing diagonal dephasing,[28,33,34] and $\mathcal{U}_{\mathbf{k}}$, representing the off-diagonal contribution, respectively.[35] Due to the complexity of the equations and the focus on relaxation processes, we did not include the Hartree-Fock renormalizations well above the band gap.

Results of the simulation are shown in Fig. 3. In Fig. 3(a), the time evolution of the energy resolved ($\hbar\omega_{\mathbf{k}} = a|\mathbf{k}|$ with $a = 0.6$ nm · eV) carrier population $f_{\mathbf{k}}(t)$ is plotted. The initial state ($t = -10$ fs) before the arrival of the pulse is a Fermi-Dirac distribution at room temperature. The calculation shows that after the optical excitation at 0.75 eV at $t = 0$ fs, the carriers in excited states are redistributed to energetically lower states resulting in a hot Fermi distribution. A detailed

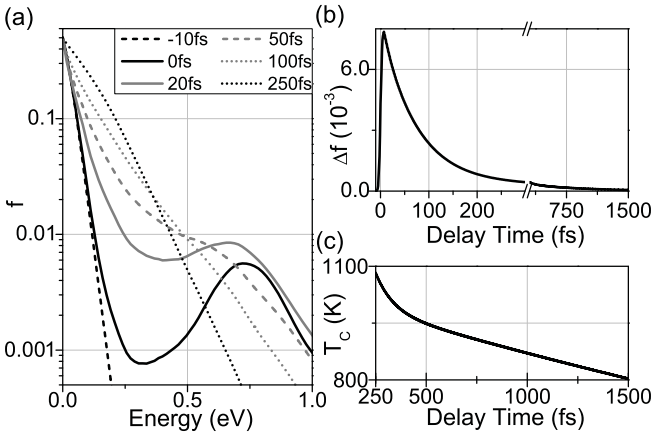

FIG. 3. (a) Calculated equilibration of carrier distribution [$f(\hbar\omega)$] due to carrier-carrier and carrier-phonon scattering. (b) Change of the carrier distribution Δf for the first picosecond integrated over the experiment's relevant energy window (0.6–0.9 eV). (c) Time evolution of the carrier temperature T_c as determined by fitting a Fermi-Dirac distribution to the simulation results.

analysis shows that this ultrafast carrier equilibration within the first 250 fs is primarily governed by electron-electron scattering, transferring carriers to lower energies. However, separate simulations of the Coulomb and the phonon-induced dynamics show that carrier-phonon scattering and hot phonon generation also considerably contribute to carrier equilibration and result in a substantial loss of excess energy to the lattice during this equilibration dynamics. The completion of the Coulomb-induced dynamics results in a slowdown of the decrease of Δf [cf. Eq. (1), Fig. 3(b)], assisted by the absorption of hot phonons by the carrier system. During the next stage in time (>250 fs), phonon-induced recombination dominates.

Thus, theory shows that the relaxation is characterized by two components, close to the data in Fig. 1(c): After establishing hot Fermi-Dirac distributions of electrons and holes (with separate quasi-Fermi levels) within 250 fs by combined action of electron-electron and electron-phonon interaction, the dynamics are determined by intra- and interband phonon-induced processes. The corresponding recombination time extracted from the theoretical calculations has a value of 2.7 ps, close to the time interval over which the negative spectrally integrated $\Delta T/T_0$ decays [Fig. 1(c)]. One possibility to explain the negative $\Delta T/T_0$ is a renormalization of electron and hole states by the transient carrier populations. More precisely, the renormalization of the single particle energies $\varepsilon^{\lambda}_{\mathbf{k}}$ by the electron-hole plasma leads to a modified $\mathbf{k}$-dispersion $\tilde{\varepsilon}^{\lambda}_{\mathbf{k}}$ of the optically coupled bands connected with a change of interband absorption $\tilde{\varepsilon}^{\lambda}_{\mathbf{k}}(t) = \varepsilon^{\lambda}_{\mathbf{k}} - \sum_{\lambda'\mathbf{k}'} V^{\lambda\lambda'\lambda'\lambda}_{\mathbf{k}\mathbf{k}'\mathbf{k}'\mathbf{k}} f^{\lambda'}_{\mathbf{k}'}(t)$, where $V^{\lambda\lambda'\lambda'\lambda}_{\mathbf{k}\mathbf{k}'\mathbf{k}'\mathbf{k}}$ is the Coulomb matrix element. We also note that another explanation discussed in literature ascribes the negative $\Delta T/T_0$ signal to thermal diffusion and shrinkage of band separation caused by lattice heating.[9,36]

At a 250 fs delay, the quasiequilibrium electron and hole distributions are characterized by a temperature $T_c \approx 1100$ K [Fig. 3(c)]. This value is much lower than the maximum possible $T_c^{\max} \approx 3600$ K estimated from the excess energy supplied by the pump pulse. This discrepancy and the initial

decrease of T_c are caused by a loss of energy, due to optical phonon emission, and by a generation of cold carriers, due to Coulomb-induced Auger processes.[26] After 500 fs, the phonon population reaches its maximum and reabsorption of hot phonons by the carrier system slows down the cooling process.

The carrier relaxation scenario in graphene is very close to that in graphite,[12] with respect to the time scale and the sequence of intraband equilibration/cooling followed by electron-hole recombination. Thus, couplings between different graphite layers play a minor role for ultrafast carrier relaxation. Even without having done explicit calculations, we believe that our theoretical treatment[26] accounts also for electron dynamics in graphite, since we checked the robustness of the dynamics for small band gaps. The improved description[26] elucidates the key role of Auger processes at early times and provides the completion of Coulomb-induced dynamics after $t_{eq} = 250$ fs as the overall equilibration time.[37]

In conclusion, ultrafast carrier relaxation in a single graphene layer has been investigated by a combined experiment-theory approach. Applying a 10-fs-time resolution, we find, as a first step, the formation of a hot Fermi-Dirac distribution within 250 fs due to carrier-carrier scattering and phonon-induced intraband processes. Afterwards, the Coulomb interaction becomes less relevant and recombination and cooling via carrier-phonon scattering proceed on a few picoseconds time scale.

We gratefully acknowledge initial help with the graphene preparation by S. Eilers, as well as financial support by the Deutsche Forschungsgemeinschaft [Sonderforschungsbereich 658 and DFG-ZUK 45/1 (C. R.)].

*elsasser@mbi-berlin.de

[1] A. K. Geim and K. S. Novoselov, Nat. Mater. **6**, 183 (2007).
[2] P. Avouris, Z. Chen, and V. Perebeinos, Nature Nanotechnol. **2**, 605 (2007).
[3] F. Xia *et al.*, Nature Nanotechnol. **4**, 839 (2009).
[4] Y.-M. Lin *et al.*, Electron. Dev. Lett. **31**, 68 (2010).
[5] R. P. Wallace, Phys. Rev. **71**, 622 (1947).
[6] J.-H. Bolotin *et al.*, Solid State Commun. **146**, 351 (2008).
[7] J.-H. Chen *et al.*, Nature Nanotechnol. **3**, 206 (2008).
[8] H. E. Romero *et al.*, ACS Nano **2**, 2037 (2008).
[9] K. Seibert, G. C. Cho, W. Kutt, H. Kurz, D. H. Reitze, J. I. Dadap, H. Ahn, M. C. Downer, and A. M. Malvezzi, Phys. Rev. B **42**, 2842 (1990).
[10] T. Kampfrath, L. Perfetti, F. Schapper, C. Frischkorn, and M. Wolf, Phys. Rev. Lett. **95**, 187403 (2005).
[11] J. M. Dawlaty *et al.*, Appl. Phys. Lett. **92**, 042116 (2008).
[12] M. Breusing, C. Ropers, and T. Elsaesser, Phys. Rev. Lett. **102**, 086809 (2009).
[13] D. Sun *et al.*, Phys. Status Solidi C **6**, 470 (2009).
[14] H. Yan, D. Song, K. F. Mak, I. Chatzakis, J. Maultzsch, and T. F. Heinz, Phys. Rev. B **80**, 121403 (2009).
[15] H. Wang *et al.*, Appl. Phys. Lett. **96**, 081917 (2010).
[16] R. D. Newson *et al.*, Opt. Express **17**, 2326 (2009).
[17] L. Huang *et al.*, Nano Lett. **10**, 1308 (2010).
[18] B. A. Ruzicka *et al.*, Appl. Phys. Lett. **96**, 173106 (2010).
[19] C. H. Lui, K. F. Mak, J. Shan, and T. F. Heinz, Phys. Rev. Lett. **105**, 127404 (2010).
[20] C. H. Lui *et al.*, Nature **462**, 339 (2009).
[21] M. Dorn *et al.*, J. Appl. Phys. **108**, 106101 (2010).
[22] C. Casiraghi *et al.*, Nano Lett. **7**, 2711 (2007).
[23] A. C. Ferrari *et al.*, Phys. Rev. Lett. **97**, 187401 (2006).
[24] L. A. Falkovsky and S. S. Pershoguba, Phys. Rev. B **76**, 153410 (2007).
[25] K. F. Mak, M. Y. Sfeir, Y. Wu, C. H. Lui, J. A. Misewich, and T. F. Heinz, Phys. Rev. Lett. **101**, 196405 (2008).
[26] T. Winzer *et al.*, Nano Lett. **10**, 4839 (2010).
[27] S. Butscher *et al.*, Appl. Phys. Lett. **91**, 203103 (2007).
[28] M. Lindberg and S. W. Koch, Phys. Rev. B **38**, 3342 (1988).
[29] E. Malic, M. Hirtschulz, F. Milde, A. Knorr, and S. Reich, Phys. Rev. B **74**, 195431 (2006).
[30] A. Grüneis, R. Saito, G. G. Samsonidze, T. Kimura, M. A. Pimenta, A. Jorio, A. G. SouzaFilho, G. Dresselhaus, and M. S. Dresselhaus, Phys. Rev. B **67**, 165402 (2003).
[31] K. Kang, D. Abdula, D. G. Cahill, and M. Shim, Phys. Rev. B **81**, 165405 (2010).
[32] M. Hirtschulz, E. Malic, F. Milde, and A. Knorr, Phys. Rev. B **80**, 085405 (2009).
[33] S. Hughes *et al.*, Solid State Commun. **100**, 555 (1996).
[34] A. Knorr *et al.*, J. Chem. Phys. **210**, 27 (1996).
[35] M. Hirtschulz, F. Milde, E. Malic, S. Butscher, C. Thomsen, S. Reich, and A. Knorr, Phys. Rev. B **77**, 035403 (2008).
[36] J. Shang *et al.*, Appl. Phys. Lett. **97**, 163103 (2010).
[37] In Ref. 12 [Fig. 1(d)], $t'_{eq} \approx 30$ fs characterizes the initial spreading of the carrier distribution.